



OPEN Hepatotoxicity evaluation method through multiple-factor analysis using human pluripotent stem cell derived hepatic organoids

Dae-Seop Shin^{1,6}, Jung Yoon Yang^{1,6}, Ha Neul Jeong^{1,2,6}, Seon Ju Mun³, Hyunwoo Kim¹, Myung Jin Son^{3,4}✉ & Myung Ae Bae^{1,2,5}✉

Prediction of the potential for drug-induced liver injury (DILI) in the early stages of drug development is important. We developed an organoid-based and functional endpoint method for accurate prediction of DILI. To this end, hepatic organoids (HOs) derived from human pluripotent stem cells (hPSCs) were cocultured with hepatic stellate cells (HSCs) and THP-1 macrophages in Matrigel domes to mimic the cellular and physiological environment of the human liver. To validate our hepatotoxicity prediction model, we selected 12 hepatotoxic reference compounds. As indicators, we used factors related to mechanisms of hepatotoxicity and markers thereof, including factors related to oxidative stress and proinflammatory cytokines. We plotted radar graphs and calculated the relative areas of polygons to analyze the effects of drugs with different degrees of hepatotoxicity. The drugs in the severe DILI group significantly increased the levels of factors related to oxidative stress (ROS, GSSH, and catalase) compared to those in the no and mild DILI groups. The drugs in the severe group significantly increased the levels of inflammation-related factors (IL-1, IL-6, and IL-10). The drugs in the mild and severe groups highly significantly increased the activities of ALT and AST and the level of ALB compared to those in the no DILI group. In summary, the drugs in the severe DILI group had significantly greater effects on the factors analyzed than those in the no DILI group. Therefore, our hepatotoxicity evaluation method is suitable for predicting DILI in the early stages of drug development.

Keywords Hepatotoxicity, Hepatic organoid, Drug-induced liver injury

It is known that approximately 20% of developed drugs have been withdrawn from the market due to drug-induced liver injury (DILI), so predicting hepatotoxicity is important in drug development¹. There is a marked difference between nonclinical and clinical findings related to DILI. Therefore, predicting the toxicity of a drug in the early stages of development is important to reduce this failure rate². Recent large-scale DILI registries have provided valuable insights into the epidemiology, risk factors, and clinical outcomes of drug-induced liver injury across different populations. The Spanish DILI Registry³, US DILI Network⁴, Latin American DILI Network⁵, and the Indian Network for DILI⁶ have contributed to the global understanding of DILI, identifying key hepatotoxic drugs and patient-specific risk factors.

DILI can be categorized into intrinsic and idiosyncratic types. Intrinsic DILI is dose-dependent and predictable, whereas idiosyncratic DILI (iDILI) is unpredictable, occurring only in a subset of individuals despite therapeutic drug doses^{7,8}. The present study focuses on iDILI, which is multifactorial in nature, involving complex interactions between host- and drug-related factors, such as genetic predisposition, environmental influences, immune system responses, and specific drug properties. Reactive oxygen species (ROS) initiated by nitric oxide (NO) play a critical role in iDILI by inducing oxidative stress, damaging liver cells, and disrupting cellular homeostasis⁹. The cellular damage associated with lipid peroxidation and nucleic acid alterations due

¹Therapeutics & Biotechnology Division, Korea Research Institute of Chemical Technology, Daejeon 34114, Republic of Korea. ²Department of Medicinal Chemistry and Pharmacology, University of Science & Technology, Daejeon 34114, Republic of Korea. ³Stem Cell Convergence Research Center, Korea Research Institute of Bioscience and Biotechnology, 125 Gwahak-ro, Yuseong-gu, Daejeon 34141, Republic of Korea. ⁴Department of Functional Genomics, University of Science & Technology, Daejeon 34113, Republic of Korea. ⁵Bio Platform Technology Research Center, Korea Research Institute of Chemical Technology, Daejeon 34114, South Korea. ⁶Dae-Seop Shin, Jung Yoon Yang and Ha Neul Jeong contributed equally to this work. ✉email: mjson@kribb.re.kr; mbae@kRICT.re.kr

to oxidative stress is a major cause of hepatotoxicity¹⁰. Additionally, Kupffer cells exposed to oxidative stress release cytokines, promoting inflammation and apoptosis, thereby exacerbating liver injury¹¹. Hepatocytes are particularly sensitive to oxidative stress compared to other non-mesenchymal cells¹², and Kupffer cells, upon activation, release pro-inflammatory cytokines and chemokines that accelerate liver damage¹³. Hepatotoxicants are known to induce iDILI by causing cytokine imbalances¹⁴. In addition to Kupffer cells, hepatic stellate cells (HSCs) also play a critical role in hepatotoxicity. HSCs are involved in liver fibrosis progression by producing extracellular matrix components and pro-fibrotic cytokines in response to liver injury. Upon activation, HSCs can exacerbate liver damage by promoting inflammation and fibrosis, which can ultimately lead to chronic liver disease¹⁵. Recent studies have highlighted the interplay between Kupffer cells and HSCs in the pathogenesis of iDILI, with activated HSCs contributing to the fibrotic response and worsening the severity of liver injury¹⁶. Furthermore, increased serum levels of IL-6 and IL-10 have been associated with the severity of liver injury, particularly in cases of drug-induced liver injury caused by anti-tuberculosis drugs¹⁷.

In vitro cell and in vivo animal models have been developed to predict hepatotoxicity during drug development. Hepatic-derived cell line such as HepG2, HepaRG and Huh have been used to predict hepatotoxicity in the early stages of drug development¹⁸. However, these immortalized cell lines have low hepatic function and drug-metabolic-enzyme activity compared to human tissue, and so cannot reflect the complex metabolic effects of drugs in vivo¹⁹. Primary human hepatocytes (PHHs) are the gold standard in vitro model for evaluating drug metabolism and toxicity²⁰. However, they have a short lifespan, show donor-derived variability, and are associated with high costs²¹. Animal models (e.g., mouse, rat, and dog) are used to evaluate drug-induced hepatotoxicity in the late stages of drug development. However, they cannot accurately recapitulate the human metabolic response to drugs because of the considerable interspecies differences in CYP-mediated drug metabolism. In addition, the use of animal models is hampered by ethics issues²².

As a result of their high availability, stem cells have been used in regenerative medicine, safety pharmacology, and toxicology. Human embryonic stem cells (hESCs) and human induced pluripotent system cells (hiPSCs) have been used to generate hepatocyte-like cells. More than 90% of hepatocytes differentiated from hESCs/hiPSCs are positive for albumin²³. Moreover, hESC-derived hepatocytes have similar patterns of gene expression and hepatotoxicity profiles to primary cultured hepatocytes²⁴. However, there is no standard method for inducing the differentiation of hESCs and hiPSCs into hepatocytes²⁵. Models based on iPSCs typically have little ability to predict hepatotoxicity because of their lesser functionality than other in vitro hepatocellular models²⁶. Three-dimensional (3D) cultures such as spheroids or organoids have superior differentiation abilities and metabolic functions compared to two-dimensional (2D) cultures of stem cells². Organoids are in vitro 3D culture systems in which cells self-organize to recapitulate tissue structure and function²⁷. Several differentiation methods have been developed to induce liver organoids that are morphologically, functionally, and genetically similar to those of liver tissue²⁸. The levels of several markers of hepatic function (e.g., albumin, α 1-antitrypsin, and cytochrome P450 enzymes) are increased in hepatic organoids (HOs) cultured in differentiation medium. Efforts to overcome the above limitations have focused on developing a more physiologically relevant in vitro hepatic model using HOs. In this study, we developed a highly efficient method for evaluating drug-induced hepatotoxicity based on factors related to oxidative stress, inflammation, and liver function.

Methodology

Culture of HOs

HOs were cultured according to the instructions of previously reported protocol²⁹. Organoid fractions were homogeneously suspended in Matrigel (Corning; 33342) and solidified as domes on cell culture plates for 15 min at 37 °C in a humidified chamber in an atmosphere of 5% CO₂. Domes were submerged in Advanced DMEM (Gibco) containing 1× N2 Supplement (Gibco), 1× B27 Supplement w/Vit A (Gibco), 100 units/mL penicillin-streptomycin (Hyclone), 1% Glutamax (Gibco), 10 mM HEPES, 1% insulin-transferrin-selenium (Gibco), 50 ng/mL human EGF (Peprotech), 25 ng/mL human HGF (Peprotech), 25 ng/mL human FGF (Peprotech), 10 ng/mL oncostatin M (R&D Systems), 5 μ M A83-01 (Tocris), 10.5 μ M forskolin (Sigma-Aldrich), 1 mM N-acetylcysteine (Sigma-Aldrich), 10 nM [Leu15]-gastrin 1 human (Sigma-Aldrich), 10 mM nicotinamide (Sigma-Aldrich), and 100 nM dexamethasone (Sigma-Aldrich). The medium was replaced every 3 days. After 7 days, the organoids were washed three times with cold medium by pipetting to remove Matrigel. The organoids were collected and fractionalized using 500 μ L Gentle Cell Dissociation Reagent (Stemcell™ Technologies) by pipetting approximately 15 times. The organoid fractions were washed three times with cold medium to eliminate Gentle Cell Dissociation Reagent and passaged at a 1: 3 ratio.

Culture of nonparenchymal cells

THP-1 (ATCC) human macrophages were obtained from the Korea Cell Line Bank (Seoul, South Korea) and were cultured in RPMI medium supplemented with 10% FBS and 100 units/mL penicillin-streptomycin solution (Hyclone). To differentiate THP-1 cells into macrophage-like cells, they were treated with 200 nM phorbol 12-myristate 13-acetate (PMA, Sigma-Aldrich) for 72, followed by a 24 h recovery period in PMA-free medium before use in co-culture³⁰. HSC stellate cells (ScienCell, #5300) were maintained in StCM (ScienCell, #5301) medium and were cultured in dishes coated with poly L-lysine according to the manufacturer's instructions.

Coculture of HOs with nonparenchymal cells

HOs were collected by washing three times with cold medium to remove Matrigel, followed by centrifugation. The HOs were treated with 0.05% Trypsin-EDTA and incubated at 37 °C for 5 min to dissociate into single cells, with gentle pipetting to achieve a homogeneous suspension. Next, they (5×10^5 cells) were mixed with THP-1 cells (1.5×10^5) and HSCs (0.5×10^5) and harvested after centrifugation. The mixture of cell types was homogeneously suspended in 1 mL Matrigel and 10 μ L aliquots were dispensed into 96-well U-bottom plates. The

plates were incubated at 37 °C for 15 min for dome formation, and 200 µL hepatic medium was gently dispensed into each well.

Treatment with hepatotoxic compounds and sampling

All compounds used in the experiment were prepared at a concentration of 20 mM using DMSO. When applied at the final test concentration, the DMSO concentration in the culture medium was maintained at 0.01%. A 0.01% DMSO-treated group was used as the control (Ctrl). On the third day after cell seeding, 100 µL of medium was removed from each well of a 96-well plate, and 100 µL of the test compound, diluted to 40 µM (twice the final concentration), was added to each well. After the plate was incubated for 9 h, 150 µL of medium was removed from each well for oxidative stress analysis. The compounds were then diluted to 20 µM in hepatic medium, and 150 µL was added to each well. After an additional 39 h of incubation, reaching a total of 48 h post-treatment, the collected medium was used for the analysis of cytokine levels and hepatic function markers. Time flow chart of experimental scheme was shown in Fig. S1.

Cell viability

Cell viability was analyzed using the CellTiter-Glo 3D Cell Viability Assay (Promega, #G9681) according to the manufacturer's instructions. Cells cultured for 2 days in 96-well plates were incubated with 3D reagent for 30 min. The mixtures were added to a 96-well white-bottom plate and luminescence was measured using a microplate reader.

Analysis of mitochondrial function

Mitochondrial function was measured using the Mitochondrial ToxGlo™ Assay (Promega, #G8000) according to the manufacturer's instructions. Cells cultured in 96-well plates for 72 h were incubated with the test compounds for 30 min. Fluorescence was measured at excitation and emission wavelengths of 485 and 520 nm, respectively, using a microplate reader. Next, ATP detection buffer was added, the mixtures were stirred for 2–3 min, and luminescence was measured using a microplate reader.

Reverse transcription-quantitative polymerase chain reaction (RT-qPCR)

Total RNA was extracted from mono- and cocultured HOs using TRIzol™ reagent (Invitrogen). mRNA levels were measured using a NanoDrop spectrophotometer (Thermo). RT-qPCR was performed with SYBR Green Real-Time PCR Master Mix (TOYOBO) in a MicroAmp™ Fast Optical 96-Well Reaction Plate sealed with MicroAmp™ Optical Adhesive Film (Life Technologies). The primer pairs were as follows: CYP1A2, forward 5'-AGCAGTCCCTCCACA-3' and reverse 5'-CATAGACACAGAAAGTAG-3'; CYP2C9, forward 5'-AGGAA AACGGATTTGTGTGG-3' and reverse 5'-GGCCATCTGCTCTTCTTCAG-3'; CYP2C19, forward 5'-GGAT TGTAAGCACCCCCTG-3' and reverse 5'-TAAAGTCCCGAGGGTTGTG-3'; CYP2D6, forward 5'-TGTGC CCATCACCAGAT-3' and reverse 5'-AAGGTGGAGACGGAGAAGC-3'; CYP3A4, forward 5'-TACACAA AAGACCGAGTGG-3' and reverse 5'-TGCAGTTTCTGCTGGACATC-3'; ALB, forward 5'-GCAAGAGAT GCCCTACATGGA-3' and reverse 5'-GGCACGAGGGGTGATGAA-3'; ALB, forward 5'-AACATGTGTTGC TATCCTGAA-3' and reverse 5'-CCTCTACCGAAGTGGGAATAAG-3'; AAT9, forward 5'-ACTGTCAACTTC GGGGACAC-3' and reverse 5'-CATGCCTAAACGCTTCATCA-3'; and β-actin forward 5'-GGACTTCGAGC AAGAGATGG-3' and reverse 5'-AGCACTGTGTTGGCGTACAG-3'. RT-qPCR was performed using Verso™ SYBR Green One-Step qRT-PCR Low ROX Mix (Thermo Scientific, Waltham, MA) on a 7500 Fast Real-Time PCR System (Applied Biosystems, Foster City, CA). mRNA levels were analyzed using the ΔΔCT method and the results were normalized to β-actin.

Measurement of ROS levels

The levels of ROS were measured using a DCFDA-based assay. Cell culture media were collected 9 h after treatment with the cytotoxic compounds, and 100 µL was transferred to Eppendorf tubes. DCFDA was added to the tubes to a final concentration of 1 µM. Next, 50 µL of the mixture was transferred to a black 384-well plate, and fluorescence was measured using excitation and emission wavelengths of 493 and 530 nm, respectively, in a microplate reader.

Measurement of catalase activity

Catalase inhibition was measured using the Catalase Activity Assay Kit (Abcam, #ab83464) according to the manufacturer's instructions. Cell supernatants after treatment with the hepatotoxic compounds for 9 h was collected and diluted fivefold with assay buffer. Test wells were assigned to the positive control, sample, and sample high control groups. Diluted cell supernatants (40 µL) were added to the wells, followed by 6 µL H₂O₂ solution. Before treatment with H₂O₂, 5 µL stop solution was added to each well. The plate was incubated at room temperature for 30 min, and 5 µL stop solution was added to the positive control and sample groups. Next, 5 µL developer mix was added to each well, and the plate was incubated for 10 min. Assay buffer, OxiRed probe, and HRP solution were mixed as the developer solution. Fluorescence was measured using a microplate reader at excitation and emission wavelengths of 535 and 587 nm, respectively.

Evaluation of the GSH/GSSG ratio

The GSH/GSSG ratio was measured using the GSH/GSSG Ratio Detection Assay Kit II (Abcam, #ab205811) according to the manufacturer's instructions. Briefly, after treatment with the hepatotoxic compounds for 9 h, cell supernatants were diluted 1:10 with assay buffer. Next, 25 µL diluted supernatants were added in triplicate to the wells of a 96-well plate. The plate was incubated at room temperature for 60 min protected from light.

Fluorescence was monitored using a microplate reader in kinetic mode at excitation and emission wavelengths of 490 and 520 nm, respectively, for 10 min.

Quantification of cytokine levels

The levels of IL-1 β , IL-6, and IL-10 were measured using the Human IL-1 β ELISA Kit (Abcam, #ab214025), Human IL-6 ELISA Kit (Abcam, #ab178013), and Human IL-10 ELISA Kit (Abcam, #ab46034), respectively, according to the manufacturers' instructions. All of the wells of a 96-well microtiter plate were coated with antibodies against IL-1 β , IL-6, and IL-10. Absorbance at 450 nm was measured using a microplate reader.

Measurement of ALT activity

The activity of ALT was measured using the Alanine Transaminase Activity Assay Kit (Abcam, #ab105134) according to the manufacturer's instructions. Cell culture media were collected and mixed 1:1 with assay buffer. Four microliters of the mixtures was added to the wells of a 384-well plate, followed by 16 μ L enzyme mixture. Fluorescence was measured at excitation and emission wavelengths of 535 and 587 nm, respectively; the 535/587 nm ratio was calculated to obtain the zero-time value. The plate was incubated for 40 min and fluorescence was measured as described above.

Measurement of AST activity

The activity of AST was quantified using the Aspartate Aminotransferase Activity Assay Kit (Abcam, #ab105135) according to the manufacturer's instructions. After adding 25 μ L cell culture media to half of the wells of a 96-well plate, 50 μ L enzyme mixture was added to each well. Absorbance was measured at a wavelength of 540 nm. The plate was incubated for 60 min and absorbance was measured as described above.

Measurement of albumin level

The level of albumin was measured using the Human Albumin ELISA Kit (Abcam, #ab108788) according to the manufacturer's instructions. Briefly, 100 μ L cell supernatant was collected after treatment with the hepatotoxic compounds for 48 h, added to a collagen-coated 96-well plate, and incubated overnight at 4°C. The wells were washed three times with 200 μ L wash buffer. Biotin conjugate was added to each well, and the plate was incubated for 1 h at room temperature, followed by three washes with 200 μ L wash buffer. The plate was incubated with gentle shaking for 45 min after adding 100 μ L streptavidin-HRP solution. After washing four times with wash buffer, 100 μ L TMB solution was added to each well and the plate was incubated for 30 min protected from light. Stop solution (50 μ L) was added, and the absorbance at 540 nm was measured.

Statistics

Each experiment was performed with a minimum of three biological replicates ($n = 3 \sim 5$), with three technical replicate per condition. Data are presented as means \pm standard errors of the mean (SEM). P values were calculated using the nonparametric unpaired t-test with Prism 8 v.8.4.3 software (GraphPad Software, CA). Statistical significance was set at 0.05 and 0.001 ($*p \leq 0.05$, $**p \leq 0.01$, and $***p \leq 0.001$). Radar plots were generated by normalizing the drug-induced changes in each factor relative to the untreated control using Excel (Microsoft, Redmond, WA, USA). The axes of the radar plots, based on the normalized values, were set to the same scale across all compounds. The relative polygon areas serve as a quantitative measure of the cumulative hepatotoxic impact of each compound, increasing with the potential severity of hepatotoxicity. This allows for the differentiation between groups with no hepatotoxicity, mild hepatotoxicity, and severe hepatotoxicity. Each polygon generated by the radar plot was converted into an image, and the relative areas of these polygons were analyzed using ImageJ software (National Institutes of Health, Bethesda, MD, USA). To facilitate a comparative assessment of the hepatotoxicity of each compound, the relative polygon areas were presented as bar graphs using Prism 8 v.8.4.3 software.

Results

Comparison of HO monoculture and HO/HHStC/THP-1 coculture

Activation of hepatic nonparenchymal cells such as endothelial cells and HSCs, and inflammatory cell infiltration, are implicated in DILI. To develop an HO culture system suitable for predicting hepatotoxicity, THP-1 cells and HSCs were cocultured with HO. The mRNA levels of liver-specific genes were examined via real-time PCR. The mRNA levels of markers of liver function—ALB and AAT (11-antitrypsin), and CYP enzymes except CYP2C19 and CYP2E1—were significantly higher in HO/HSC/THP-1 coculture than in monoculture (Fig. 1a). In coculture, the CYP1A2, CYP3A4, and albumin levels were increased 3.8-, 5.5-, and 5-fold, respectively. The protein levels of hepatic function-related factors were measured in cell lysate and culture medium. The ALT, AST, and urea levels did not differ between coculture and monoculture (Fig. 1b). Oxidative stress affects cell membranes, proteins, and DNA, leading to cell death, ultimately causing liver dysfunction. Because the liver is vulnerable to oxidative stress, it has been suggested that continuous oxidative stress is important in the onset and progression of liver diseases. Changes in factors associated with oxidative stress and inflammation were compared in HO monoculture and coculture of HO/HSCs/THP-1. In coculture, GSSG and catalase activities were significantly decreased and increased, respectively (Fig. 1c). Therefore, homeostasis of factors related to oxidative stress may be changed in HO/HSC/THP-1 coculture. In addition, the levels of IL-6 and IL-10 were significantly increased in coculture (Fig. 1d). Therefore, inflammation-related factors are functional in THP-1 cells in coculture. We used HO/HSC/THP-1 coculture in subsequent experiments to establish a hepatotoxicity-evaluation method based on HOs.

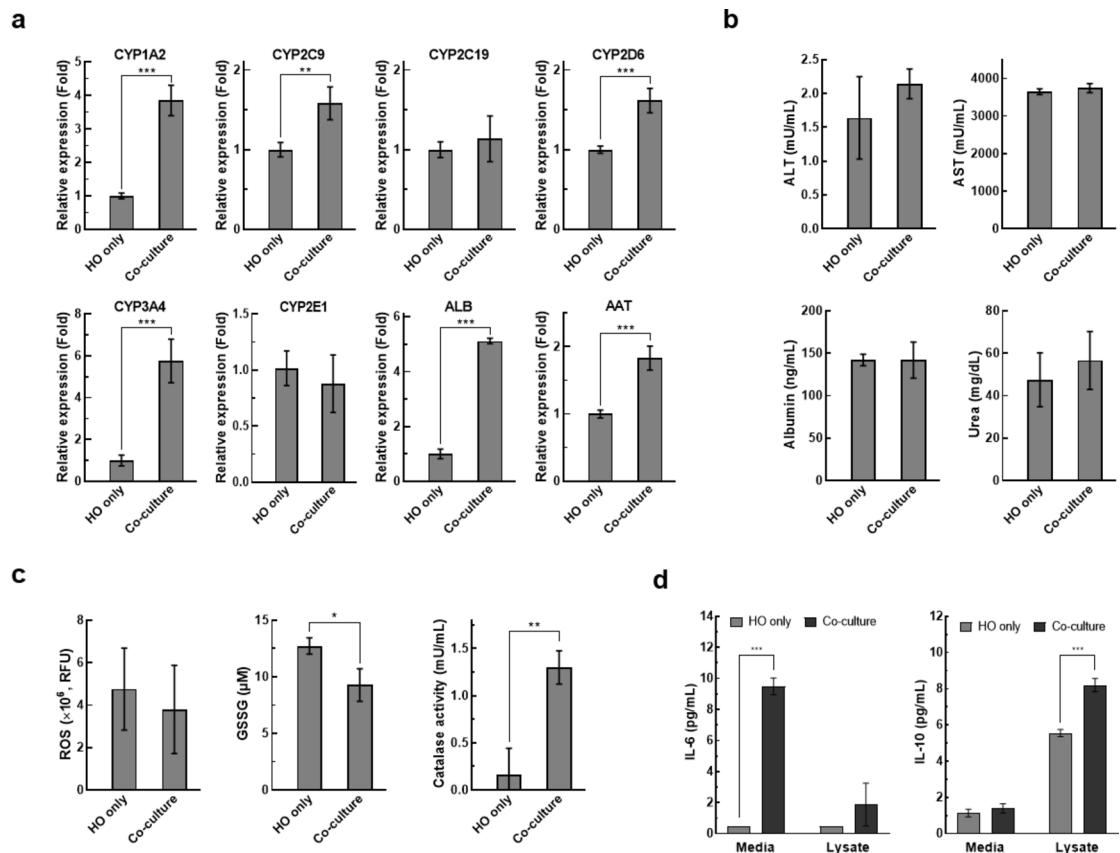


Fig. 1. Levels of factors in mono- and coculture systems. (a) mRNA levels of CYP enzymes and hepatocyte function-related factors. (b) Protein levels of factors related to hepatic function in culture medium. (c) Levels of markers of oxidative stress. (d) Levels of cytokines. Data were expressed as the means \pm standard error ($n = 3$). The statistical significance was assessed using the nonparametric unpaired t -test (* $p < 0.05$, ** $p < 0.01$, and *** $p < 0.001$).

Category	Compounds	Target disease
No DILI	Ambrisentan (AMB) ³¹	Pulmonary hypertension
	Buspirone (BUSP) ³²	Anxiety disorder
	Flumazenil (FMZ) ³³	Antiseizure
	Orphenadrine (ORP) ³⁴	Anticholinergic drug
High DILI	Azathioprine (AZA) ³⁵	Immunosuppressant
	Clozapine (CZ) ³⁶	Antipsychotic agent
	Imipramine (IMI) ³⁷	Antidepressant
	Ticlopidine (TP) ³⁸	Antiplatelet drug
Severe DILI	Amiodarone (AMIO) ³⁹	Arrhythmia
	Ketoconazole (KET) ⁴⁰	Antifungal
	Nefazodone (NEF) ⁴¹	Anti-depressant
	Troglitazone (TZ) ⁴²	Type II diabetes

Table 1. Drugs used for the evaluation of hepatotoxicity prediction model.

Mitochondrial function and cell viability

As shown in Table 1, we used 12 compounds to verify the hepatotoxicity-evaluation model. The liver is the most important organ involved in maintaining energy homeostasis, controlling the storage and metabolism of nutrients, and detoxifying blood. The mitochondria of hepatocytes, which are the most common hepatic cell type, play key roles in these biochemical processes and mitochondrial dysfunction is a mechanism of DILI. Cocultured HO/HSC/THP-1 cells were treated with the reference compounds at 20 μ M for 9 h, and mitochondrial dysfunction was analyzed. The concentration of 20 μ M was selected based on previous studies using 3D hepatic models to ensure standardized conditions for evaluating hepatotoxicity²⁶. Interestingly, only

amiodarone significantly decreased mitochondrial function (Fig. 2a). Because mitochondria generate ATP, their activity in hepatocytes is directly related to cell survival. FMZ and ORP decreased mitochondrial activity by 20% in the no DILI group; CZ, IMI, and TP decreased it by 20–30% in the mild DILI group; and KET and NEF decreased mitochondrial activity by 30% in the severe DILI group (Fig. 2b). Amiodarone inhibited cell viability by approximately 80%. In addition, it had the greatest inhibitory effect on mitochondrial dysfunction, which may explain its effect on cell survival. However, the effects of the other compounds suggested a weak correlation between mitochondrial dysfunction and cell viability. These results suggest that predicting the hepatotoxicity of drugs based solely on mitochondrial toxicity or inhibition of cell viability is not feasible. Cytotoxicity is caused by oxidative stress, and pharmaceutical-related liver disease involves a severe inflammatory response together with oxidative stress.

The selection of reference compounds was based on previously established hepatotoxicity classifications in the literature. The compounds were chosen to represent a diverse range of pharmacological classes and hepatotoxicity severity levels. Positive and negative controls were selected to validate the model's predictive capability, and future studies will incorporate additional reference compounds to further strengthen model validation.

Levels of factors related to oxidative stress

Measurement of the levels of factors related to oxidative stress can provide insight into hepatotoxicity and enable the early detection and prevention of liver damage. Thus, we measured the levels of such factors 9 h after treatment with the hepatotoxic compounds. All compounds significantly increased ROS levels by more than twofold compared to controls (Fig. 3a). The activity of catalase, which converts H_2O_2 , an agent of oxidative stress, to water and oxygen, was decreased by the compounds, particularly ORP, IMI, and TP (> 60% decrease in ROS level). Among the four hepatotoxic compounds in the severe DILI group, KET, NEF, and TZ significantly altered ROS levels, as shown in Fig. 3b. The degrees of inhibition of catalase activity significantly differed among the 12 hepatotoxic compounds. Finally, we measured the levels of GSSG, a critical component of cellular redox balance, which is generated by the reaction between GSH and ROS under oxidative stress. Its levels significantly differed according to the compound used, particularly in the severe group (Fig. 3c). To evaluate the effects of oxidative stress induced by hepatotoxic compounds, we plotted radar graphs and compared the relative areas of the polygons among the DILI groups (Fig. 3d). The relative areas of the compounds in the severe group were significantly greater than those in the no and high DILI groups (Fig. 3e, f). Therefore, DILI-causing drugs are associated with oxidative stress and their toxicity can be predicted based on parameters related to oxidative stress.

Levels of inflammatory cytokines

Hepatotoxins induce a cytokine imbalance. Treatment with the 12 hepatotoxic compounds increased the levels of IL-1 β , IL-6, and IL-10 compared to the vehicle control, and the increases caused by IMI, KET, NET, and TZ were particularly notable (Fig. 4a). The level of IL-6 was significantly increased by treatment with CZ, IMI, KET, and TZ (Fig. 4b). The level of IL-10 was significantly increased 2.36- and 3.43-fold by amiodarone and NEF, respectively, compared to the vehicle control (Fig. 4c). The levels of inflammation-related cytokines were significantly increased by several of the drugs in the mild and severe DILI groups but none of those in the no DILI group. A radar graph showed that the polygons formed by drugs in the severe DILI group were skewed towards IL-1 β and IL-10 (Fig. 4d). Furthermore, the drugs in the severe DILI group exhibited significantly larger polygon areas than those in the no DILI and mild DILI groups (Fig. 4e, f). Therefore, analysis of the above inflammatory factors enables the identification of drugs with the potential to cause severe DILI.

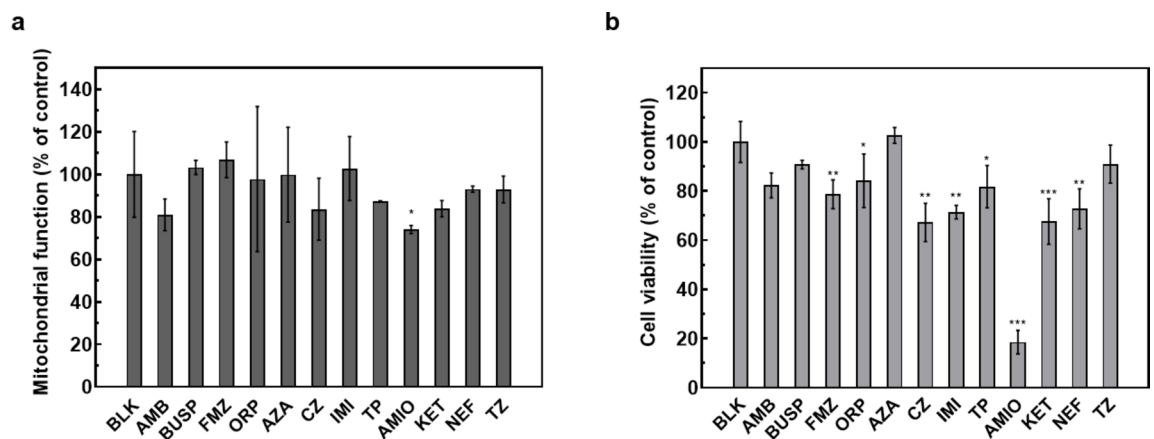


Fig. 2. Cell viability and mitochondrial dysfunction. **(a)** Cell viability rates in liver organoids and nonparenchymal cell coculture. **(b)** Mitochondrial dysfunction in liver organoids and nonparenchymal cell coculture. Data were expressed as the means \pm standard error ($n = 5$). The statistical significance was assessed using the nonparametric unpaired t -test (* $p < 0.05$, ** $p < 0.01$, and *** $p < 0.001$).

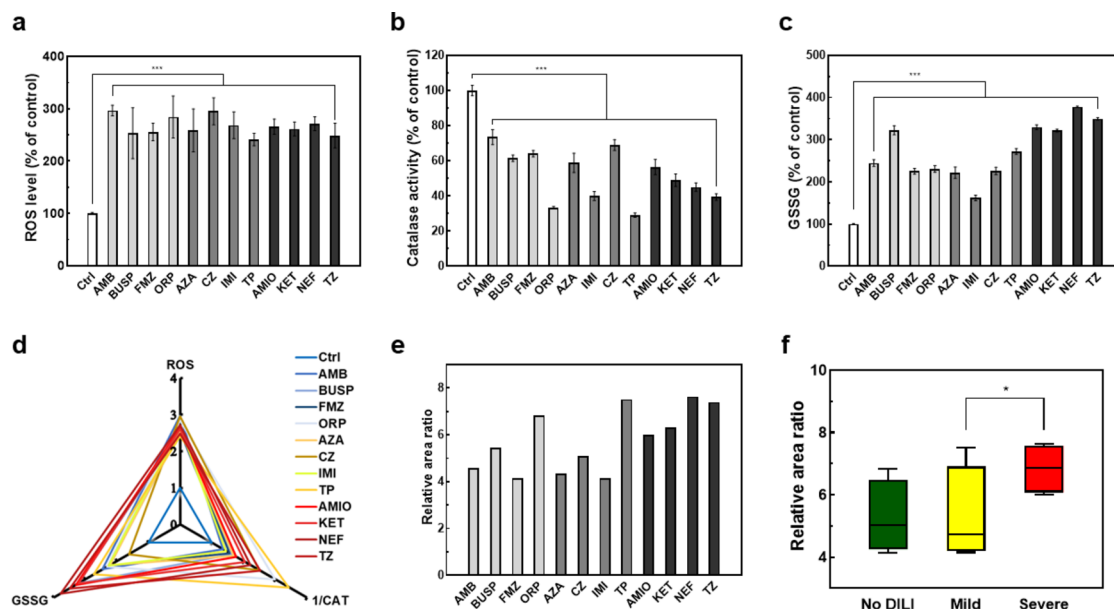


Fig. 3. Levels of factors related to oxidative stress. (a) ROS levels. (b) Catalase activity. (c) GSSG levels. (d) Radar graph of ratios to the untreated control. (e) Relative areas of polygons relative to the untreated control calculated using ImageJ software. (f) Statistical analysis of area ratios. Data were expressed as the means \pm standard error ($n = 3 \sim 5$). The statistical significance was assessed using the nonparametric unpaired t -test (* $p < 0.05$ and *** $p < 0.001$).

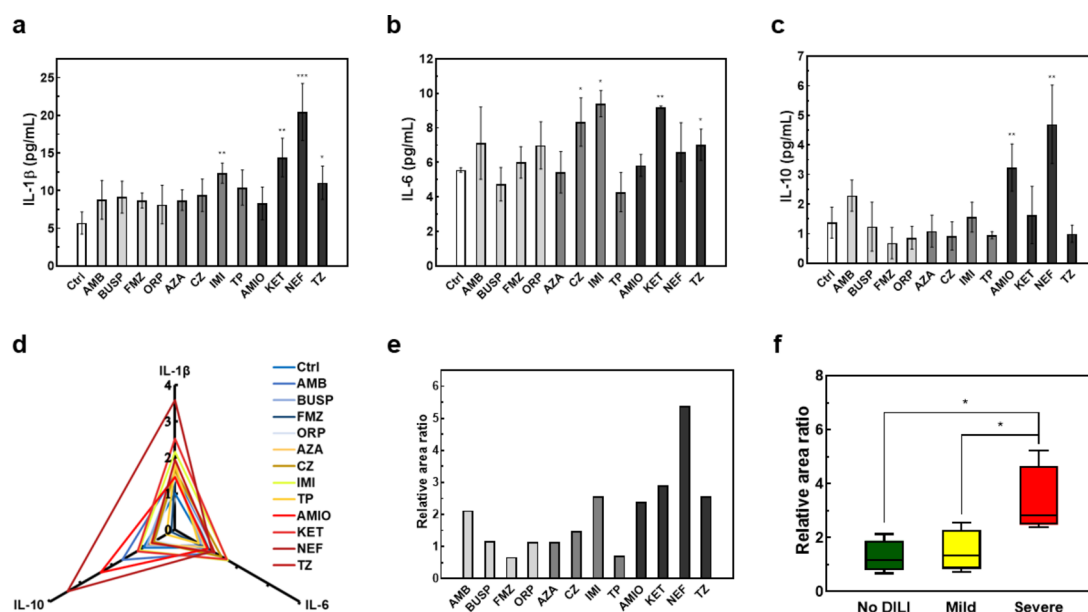


Fig. 4. Levels of pro-inflammatory cytokines. (a) IL-1 β . (b) IL-6. (c) IL-10. (d) Radar graph of ratios to the untreated control. (e) Relative area ratios of polygons to that of the untreated control calculated using ImageJ software. (f) Statistical analysis of area ratios. Data were expressed as the means \pm standard error ($n = 3 \sim 5$). The statistical significance was assessed using the nonparametric unpaired t -test (* $p < 0.05$, ** $p < 0.01$, and *** $p < 0.001$).

Levels of markers of hepatic function

Hepatic toxicity results in elevations of the levels of ALT, AST, alkaline phosphatase (ALP), and total bilirubin. These, together with albumin, triglycerides, cholesterol, and urea, are used as indicators of hepatic function. The activity of ALT was significantly increased by the hepatotoxic compounds in the mild and severe DILI groups but not those in the no DILI group (Fig. 5a). The activity of AST was unaffected by the hepatotoxic compounds in the no DILI group, except for ORP. However, more than half of the hepatotoxic compounds in the mild and

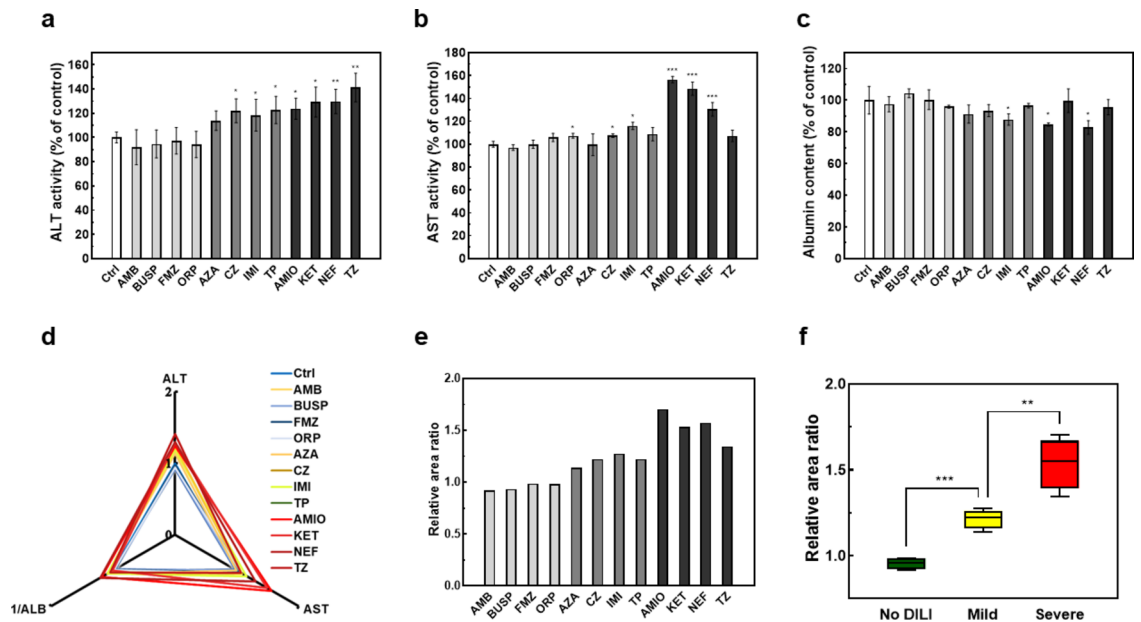


Fig. 5. Levels of factors related to liver function. (a) ALT activity. (b) AST activity. (c) Albumin levels. (d) Radar graph of ratios to the untreated control. (e) Relative polygon area ratios to that of the untreated control calculated using ImageJ software. (f) Statistical analysis of area ratios. Data were expressed as the means \pm standard error ($n = 3 \sim 5$). The statistical significance was assessed using the nonparametric unpaired t -test ($*p < 0.05$, $**p < 0.01$, and $***p < 0.001$).

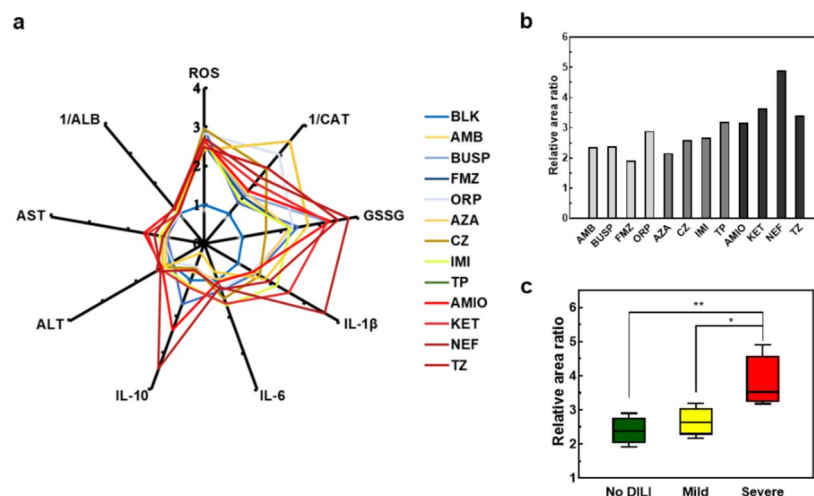


Fig. 6. Summary. (a) Radar graph of ratios compared to the untreated control. (b) Relative polygon area ratios to that of the untreated control calculated using ImageJ software. (c) Statistical analysis of area ratios. Data were expressed as the means \pm standard error ($n = 3$). The statistical significance was assessed using the nonparametric unpaired t -test ($*p < 0.05$ and $***p < 0.001$).

severe DILI groups significantly increased AST activity, particularly AMIO, KET, and NEF in the severe DILI group (Fig. 5b). The hepatotoxic compounds in the no DILI group did not significantly affect the albumin level. However, IMI (mild DILI group) and AMIO and NEF (severe DILI group) significantly decreased the albumin level (Fig. 5c). We generated radar graphs and measured polygon areas (Fig. 5d); the results indicated that the hepatotoxic compounds significantly altered the levels of markers of hepatic function, suggesting their utility for assessing hepatotoxicity (Fig. 5e, f).

Prediction of hepatotoxicity

We generated a polygon graph of the effects of the hepatotoxic compounds on oxidative stress, immune-related factors, and liver function markers. Most compounds increased the levels of factors related to oxidative stress (Fig. 6a). The polygon areas were calculated as a ratio to that of the untreated control (Fig. 6b). The polygon areas

of all hepatotoxic compounds, irrespective of their hepatotoxicity class, were greater than the untreated control; the compounds in the mild and severe DILI groups had more than twofold greater polygon areas. There were no significant differences in the polygon areas of the hepatotoxic compounds in the no and mild DILI groups (Fig. 6c). However, the compounds in the severe DILI group had significantly greater polygon areas than those in the no and mild DILI groups. These results are in agreement with those related to oxidative stress, inflammatory, and hepatic function factors. Therefore, our multifactor hepatotoxicity prediction method shows potential for predicting hepatotoxicity.

Discussion and conclusion

Predicting the toxicity of drug candidates in the early stages of drug development is important. Developing methods to accurately predict the toxicity of potential drug candidates can reduce costs by preventing the withdrawal of drugs from the market, the leading cause of which is hepatotoxicity. Therefore, accurate prediction of hepatotoxicity is a vital part of drug development. Primary human hepatocytes are the gold standard for drug metabolism and toxicity studies but have a short lifespan, high variability, and limited availability⁴³. For these reasons, animal models, murine hepatocytes, hepatoma cell lines, and immortalized hepatocytes have been used to predict drug hepatotoxicity^{44,45}. However, animal models or models using animal-derived hepatocytes do not accurately recapitulate human liver physiology. Cell-based in vitro models typically used to evaluate hepatotoxicity are based on monocultures of HepG2 and HepaRG cells. However, HepaRG cells maintain a stable metabolic phenotype but have little expression of the genes encoding CYP2E1 and glutathione transferase A1. These monoculture models also have a limited experimental window due to rapid loss of metabolic activity, typically within 48 h of drug treatment, a crucial period for accurate prediction of hepatotoxicity.

The use of alternative sources of human hepatocytes, such as hPSC-derived hepatocytes, has potential for toxicology testing in drug development. We developed a method for differentiating HOs from hPSCs, and the organoids exhibited high liver functionality²⁹. We developed a system for accurately predicting drug-induced hepatotoxicity in the early stages of drug development using hPSC-derived HOs. The hPSC-derived hepatocytes used in this study have limitations for simulating the biological and physical environment of the human liver due to the absence of Kupffer cells, hepatic stellate cells, and sinusoidal endothelial cells. According to previous research results, it has been shown that these cells in liver tissue play a significant role in the process of DILI⁴⁶. Therefore, we designed a system to enhance drug-induced inflammation and recapitulate the liver-disease environment based on coculture of THP-1 macrophages and HSC cells with HOs. Interestingly, the mRNA levels of most of the factors related to metabolism and liver function were significantly higher in coculture. However, the protein levels of liver function-related factors were not increased in coculture.

While the HO/HSC/THP-1 coculture model improves the physiological relevance of hepatotoxicity screening, it has certain limitations. The absence of liver sinusoidal endothelial cells (LSECs) and biliary epithelial cells restricts the model's ability to fully mimic the in vivo liver microenvironment. Additionally, while hepatic organoids exhibit key liver-specific functions, their metabolic activity and enzyme expression may not fully match those of primary hepatocytes, leading to potential differences in drug metabolism. The activation state of HSCs and THP-1 macrophages may also not completely reflect the dynamic progression of liver fibrosis and inflammation. Furthermore, variability in organoid size, matrix composition, and culture conditions introduces challenges in standardization and reproducibility. The model effectively captures oxidative stress-related hepatotoxicity but may have limitations in predicting toxicity mechanisms primarily mediated by mitochondrial dysfunction or direct hepatocellular damage. Inflammatory markers, such as IL-6 and IL-10, were significantly elevated only for specific hepatotoxicants, suggesting that inflammation alone may not be a universal predictor of DILI. Despite these limitations, the coculture model provides valuable insights into inflammation-driven liver injury and can be further optimized by incorporating additional liver cell types and metabolic activity assessments. Additionally, our model has limitations related to the short-term nature of the experiments, which may not fully capture chronic hepatotoxicity or delayed toxic responses. Another critical limitation is the inter-donor variability of hPSC-derived hepatocytes, which can influence drug metabolism and toxicity outcomes. Furthermore, batch-to-batch variability in organoid differentiation presents a challenge for reproducibility, potentially affecting the consistency of hepatotoxicity predictions. Future studies should focus on optimizing differentiation protocols and extending experimental timelines to enhance the reliability and predictive power of our model.

It is important to assess CYP enzyme activity in addition to mRNA expression levels when predicting hepatotoxicity. Other studies reported a strong correlation between CYP mRNA expression and enzymatic activity in hPSC-derived hepatic organoids^{24,26}. These studies have shown that the mRNA expression of CYP enzymes is a reliable indicator of their enzymatic function, which can play a crucial role in drug metabolism and hepatotoxicity assessment. Our previous study measured not only the mRNA levels of key CYP isoforms, including CYP3A4, but also their enzymatic activity, confirming that CYP3A4 activity was higher in HOs than in 2D-differentiated mature hepatocytes²⁹. In future studies, we plan to further validate and refine our hepatotoxicity prediction model by incorporating direct enzymatic assays to enhance its accuracy and strengthen its applicability in early-stage drug development for hepatotoxicity screening.

The liver is the most important organ in maintaining energy homeostasis, controlling the storage and metabolism of nutrients, and performing detoxification of blood. Previous studies provided information on their relevance to liver disease and their potential use in the prediction and monitoring of hepatotoxicity⁴⁷. It had been known that the mitochondria of hepatocyte, the highest proportion of cell species in the liver, play key roles in each of these biochemical events⁴⁸ and mitochondrial dysfunction is known to be one of the major mechanisms of DILI⁴⁹. Mitochondrial dysfunction was used for the evaluation of drug-induced hepatotoxicity⁵⁰. We measured the effects of reference compounds on mitochondrial function and cell viability (Fig. 2). Mitochondrial function was unsuitable for predicting the hepatotoxicity of the 12 compounds (except AMIO) based on the absence

of significant effects. Many of the compounds significantly modulated cell viability, including those in the no and mild DILI groups. TZ (severe DILI group) did not significantly decrease cell viability, suggesting that this parameter is unsuitable for predicting hepatotoxicity, particularly for highly hepatotoxic drugs.

In addition, the other studies have shown that liver toxicity is caused by oxidative stress, and pharmaceutical liver disease in particular is known to cause a significant inflammatory response along with oxidative stress⁵¹. Since the liver is very vulnerable to oxidative stress, it has been suggested that continuous oxidative stress plays an important role in the onset and progression of liver diseases⁵². Measuring oxidative stress-related factors can provide insight into potential hepatotoxicity and help in the early detection and prevention of liver damage. Therefore, in this study, we developed a multifactor hepatotoxicity prediction method based on coculture and measurement of the levels of several oxidative stress and inflammatory response-related factors associated with the mechanisms of drug-induced hepatotoxicity. In coculture, the level of GSSG significantly decreased and the catalase activity significantly increased, suggesting the utility of coculture for evaluating hepatotoxicity. These results indicate that co-culturing hepatic organoids with other cell types has a clear impact on various factors. Therefore, we concluded that coculture conditions would be advantageous for evaluating hepatotoxicity using various factors and used this system in the study.

Oxidative stress is associated with drug-induced hepatotoxicity and causes oxidative damage by inhibiting the antioxidant defense system, leading to inflammation, cell damage, and in severe cases, cell death. All of the hepatotoxic compounds increased ROS levels more than twofold 9 h after treatment (Fig. 3). In previous studies, IL-1 and IL-6 were used as biomarkers for acute or chronic hepatotoxicity, and mediate the hepatic response to xenobiotics such as acetaminophen and phenobarbitone⁵³. It has been also reported that hepatotoxicants induce cytokine imbalance in response to the innate immune system¹⁴. Use of IL-10, an anti-inflammatory cytokine, for hepatotoxicity prediction may be controversial. However, high levels of IL-10 in the plasma of patients with hepatitis-related hepatocellular carcinoma have been reported⁵⁴. Therefore, IL-10 was chosen as an inflammatory factor in this study, as it is believed to be useful as a biomarker for inflammation related to hepatitis or liver diseases. The 12 hepatotoxic compounds had different effects on the levels of cytokines; the levels of IL-1 β and IL-10 were significantly increased by NEF (severe DILI group). However, we acknowledge that the levels of inflammatory factors were notably elevated only in response to NEF, while other compounds did not induce a comparable increase (Fig. 4e). This variability may be attributed to differences in the mechanisms of hepatotoxicity among drugs. While some hepatotoxicants induce inflammation-mediated liver injury, others may primarily exert toxicity through oxidative stress, mitochondrial dysfunction, or direct hepatocellular damage. Therefore, our results suggest that inflammatory markers alone may not be sufficient to comprehensively predict severe DILI but should be considered in conjunction with other hepatotoxicity indicators. The compounds used in this study represent a range of hepatotoxic mechanisms, which is crucial for validating the predictive power of our model. AMIO and TZ are known to cause mitochondrial dysfunction, leading to hepatocellular injury. KET and NEF inhibit bile acid transporters, contributing to cholestatic liver injury. AZA and CZ induce hepatotoxicity through immune-mediated mechanisms, leading to liver inflammation and idiosyncratic DILI. In contrast, IMI and TP are associated with reactive metabolite formation and oxidative stress, further contributing to hepatocyte damage. The inclusion of these mechanistically diverse compounds strengthens our model by ensuring its applicability to various forms of hepatotoxicity. However, while our model effectively captures inflammation- and oxidative stress-driven toxicity, its ability to predict cholestatic or purely metabolic injury requires further validation. Future studies should incorporate additional compounds with well-defined hepatotoxic pathways to enhance mechanistic coverage.

It is important to note that while drugs classified under the “No DILI” category, such as buspirone and flumazenil, have been generally considered non-hepatotoxic, rare cases of hepatotoxicity have been reported⁵⁵. This highlights the complexity of DILI classification and the potential influence of genetic, environmental, and metabolic factors on individual susceptibility to drug-induced hepatotoxicity. These findings emphasize the need for continuous refinement of hepatotoxicity prediction models using expanded reference compound datasets. The hepatotoxic compounds in the severe DILI group significantly increased the levels of the three cytokines compared to those in the no and mild DILI groups (Fig. 4f), suggesting that the levels of proinflammatory cytokines can be used to identify drugs that cause severe DILI.

Hepatic toxicity is characterized by ALT, AST, and alkaline phosphatase (ALP), total bilirubin (TBILI), these are most basic and widely used markers to evaluate liver function⁵⁶. Several biomarkers like albumin, triglycerides, cholesterol and urea is considered to be supplemental indicators of hepatic function⁵⁷. Based on previous in vitro tests, we aimed to quantify hepatic function markers to predict hepatotoxicity⁵⁸. Interestingly, the activities of ALT and AST were significantly increased by the hepatotoxic compounds in the severe DILI group. Therefore, our model accurately predicts drug hepatotoxicity. hPSC-derived hepatocytes are abundant, facilitating large-scale hepatotoxicity testing. Furthermore, use of hepatocytes derived from PSCs enables the establishment of patient-specific models. In conclusion, our hepatotoxicity prediction model represents a paradigm shift in in vitro drug hepatotoxicity screening, particularly when combined with high-throughput or high-efficiency screening systems, and will promote the development of next-generation therapies. Furthermore, our hepatotoxicity prediction model may contribute to bridging the gap between preclinical and clinical assessments of DILI. The integration of data from global DILI registries, such as the Spanish DILI Registry³ and the US DILI Network⁴, with our organoid-based screening platform could enhance its predictive accuracy and clinical relevance. Future studies should aim to validate our model against known hepatotoxicants identified in these registries.

Data availability

The data that support the findings of this study are available on request from the corresponding author. The data are not publicly available due to privacy or ethical restrictions.

Received: 25 December 2024; Accepted: 19 March 2025

Published online: 28 March 2025

References

- Onakpoya, I. J. et al. Post-marketing withdrawal of 462 medicinal products because of adverse drug reactions: a systematic review of the world literature. *BMC Med.* **14** <https://doi.org/10.1186/s12916-016-0553-2> (2016).
- Underhill, G. H. & Khetani, S. R. Bioengineered liver models for drug testing and cell differentiation studies. *Cell. Mol. Gastroenterol. Hepatol.* **5**, 426–439.e421. <https://doi.org/10.1016/j.jcmgh.2017.11.012> (2018).
- Stephens, C. et al. Comprehensive analysis and insights gained from long-term experience of the Spanish DILI registry. *J. Hepatol.* **75**, 86–97. <https://doi.org/10.1016/j.jhep.2021.01.029> (2021).
- Chalasani, N. et al. Features and outcomes of 899 patients with drug-induced liver injury: the DILIN prospective study. *Gastroenterology* **148**, 1340–1352.e1347. <https://doi.org/10.1053/j.gastro.2015.03.006> (2015).
- Bessone, F. et al. When the creation of a consortium provides useful answers: experience of the Latin American DILI network (LATINDILIN). *Clin. Liver Dis. (Hoboken)*. **13**, 51–57. <https://doi.org/10.1002/cld.778> (2019).
- Devarbhavi, H. et al. The Indian network of drug-induced liver injury: etiology, clinical features, outcome and prognostic markers in 1288 patients. *J. Clin. Exp. Hepatol.* **11**, 288–298. <https://doi.org/10.1016/j.jceh.2020.11.002> (2021).
- Chen, J. et al. Recent progress in fluorescent sensors for drug-induced liver injury assessment. *ACS Sens.* **6**, 628–640. <https://doi.org/10.1021/acssensors.0c02343> (2021).
- Villanueva-Paz, M. et al. Oxidative stress in Drug-Induced liver injury (DILI): from mechanisms to biomarkers for use in clinical practice. *Antioxidants*. **10**. <https://doi.org/10.3390/antiox10030390> (2021).
- Sánchez-Valle, V. et al. Role of oxidative stress and molecular changes in liver fibrosis: a review. *Curr. Med. Chem.* **19**, 4850–4860. <https://doi.org/10.2174/092986712803341520> (2012).
- Lata, S. et al. Evaluation of the antioxidant and hepatoprotective effect of phyllanthus fraternus against a chemotherapeutic drug cyclophosphamide. *Appl. Biochem. Biotechnol.* **173**, 2163–2173. <https://doi.org/10.1007/s12010-014-1018-8> (2014).
- Rezzani, R. & Franco, C. Liver, oxidative stress and metabolic syndromes. *Nutrients* **13** <https://doi.org/10.3390/nu13020301> (2021).
- Farzaei, M. H. et al. Curcumin in liver diseases: A systematic review of the cellular mechanisms of oxidative stress and clinical perspective. *Nutrients* **10** <https://doi.org/10.3390/nu10070855> (2018).
- Surjit, M. et al. Widespread negative response elements mediate direct repression by agonist-liganded glucocorticoid receptor. *Cell* **145**, 224–241. <https://doi.org/10.1016/j.cell.2011.03.027> (2011).
- Goto, S. et al. Hepatotoxicants induce cytokine imbalance in response to innate immune system. *J. Toxicol. Sci.* **40**, 389–404. <https://doi.org/10.2131/jts.40.389> (2015).
- Battaller, R. & Brenner, D. A. Liver fibrosis. *J. Clin. Invest.* **115**, 209–218. <https://doi.org/10.1172/JCI24282> (2005).
- Geng, Y. et al. Hepatic stellate cells induce an inflammatory phenotype in Kupffer cells via the release of extracellular vesicles. *J. Cell. Physiol.* **238**, 2293–2303. <https://doi.org/10.1002/jcp.31086> (2023).
- Xiang, H. R. et al. Serum levels of IL-6/IL-10/GLDH May be early recognition markers of anti-tuberculosis drugs (ATB) -induced liver injury. *Toxicol. Appl. Pharmacol.* **475**, 116635. <https://doi.org/10.1016/j.taap.2023.116635> (2023).
- Deng, J. et al. Engineered liver-on-a-chip platform to mimic liver functions and its biomedical applications: A review. *Micromachines (Basel)*. **10** <https://doi.org/10.3390/mi10100676> (2019).
- Ide, I. et al. A novel evaluation method for determining drug-induced hepatotoxicity using 3D bio-printed human liver tissue. *Toxicol. Mech. Methods*. **30**, 189–196. <https://doi.org/10.1080/15376516.2019.1686795> (2020).
- Vinken, M. & Hengstler, J. G. Characterization of hepatocyte-based in vitro systems for reliable toxicity testing. *Arch. Toxicol.* **92**, 2981–2986. <https://doi.org/10.1007/s00204-018-2297-6> (2018).
- Guo, L. et al. Similarities and differences in the expression of drug-metabolizing enzymes between human hepatic cell lines and primary human hepatocytes. *Drug Metab. Dispos.* **39**, 528–538. <https://doi.org/10.1124/dmd.110.035873> (2011).
- Van Norman, G. A. Limitations of animal studies for predicting toxicity in clinical trials: is it time to rethink our current approach?? *JACC Basic. Transl. Sci.* **4**, 845–854. <https://doi.org/10.1016/j.jacbs.2019.10.008> (2019).
- Hay, D. C. et al. Highly efficient differentiation of hESCs to functional hepatic endoderm requires activina and Wnt3a signaling. *Proc. Natl. Acad. Sci. U S A*. **105**, 12301–12306. <https://doi.org/10.1073/pnas.0806522105> (2008).
- Kim, J. H. et al. Prediction of hepatotoxicity for drugs using human pluripotent stem cell-derived hepatocytes. *Cell. Biol. Toxicol.* **34**, 51–64. <https://doi.org/10.1007/s10565-017-9392-y> (2018).
- Kajiwar, M. et al. Donor-dependent variations in hepatic differentiation from human-induced pluripotent stem cells. *Proc. Natl. Acad. Sci. U S A*. **109**, 12538–12543. <https://doi.org/10.1073/pnas.1209979109> (2012).
- Bell, C. C. et al. Transcriptional, functional, and mechanistic comparisons of stem Cell-Derived hepatocytes, HepaRG cells, and Three-Dimensional human hepatocyte spheroids as predictive in vitro systems for Drug-Induced liver injury. *Drug Metab. Dispos.* **45**, 419–429. <https://doi.org/10.1124/dmd.116.074369> (2017).
- Broutier, L. et al. Culture and establishment of self-renewing human and mouse adult liver and pancreas 3D organoids and their genetic manipulation. *Nat. Protoc.* **11**, 1724–1743. <https://doi.org/10.1038/nprot.2016.097> (2016).
- Broutier, L. et al. Human primary liver cancer-derived organoid cultures for disease modeling and drug screening. *Nat. Med.* **23**, 1424–1435. <https://doi.org/10.1038/nm.4438> (2017).
- Mun, S. J. et al. Generation of expandable human pluripotent stem cell-derived hepatocyte-like liver organoids. *J. Hepatol.* **71**, 970–985. <https://doi.org/10.1016/j.jhep.2019.06.030> (2019).
- Daigneault, M. et al. The identification of markers of macrophage differentiation in PMA-stimulated THP-1 cells and monocyte-derived macrophages. *PLoS One*. **5**, e8668. <https://doi.org/10.1371/journal.pone.0008668> (2010).
- Patel, K. R. et al. Hepatic safety of ambrisentan alone and in combination with Tadalafil: a post-hoc analysis of the AMBITION trial. *Pulm Circ.* **8**, 2045894018797273. <https://doi.org/10.1177/2045894018797273> (2018).
- Kostrubsky, S. E. et al. Inhibition of hepatobiliary transport as a predictive method for clinical hepatotoxicity of nefazodone. *Toxicol. Sci.* **90**, 451–459. <https://doi.org/10.1093/toxsci/kfj095> (2006).
- Bozoglu, E. et al. The effect of different doses of Flumazenil on acetaminophen toxicity in rats. *Bratislav Lek Listy*. **113**, 525–528. https://doi.org/10.4149/bll_2012_118 (2012).
- Chou, R. et al. Comparative efficacy and safety of skeletal muscle relaxants for spasticity and musculoskeletal conditions: a systematic review. *J. Pain Symptom Manage.* **28**, 140–175. <https://doi.org/10.1016/j.jpainsymman.2004.05.002> (2004).
- Horning, K. & Schmidt, C. Azathioprine-Induced rapid hepatotoxicity. *J. Pharm. Technol.* **30**, 18–20. <https://doi.org/10.1177/8755122513504078> (2014).
- Brown, C. A. et al. Clozapine toxicity and hepatitis. *J. Clin. Psychopharmacol.* **33**, 570–571. <https://doi.org/10.1097/JCP.0b013e3182946586> (2013).
- Klerman, G. L. & Cole, J. O. Clinical pharmacology of imipramine and related antidepressant compounds. *Pharmacol. Rev.* **17**, 101–141 (1965).
- Halegoua-De Marzio, D. & Navarro, V. J. Chap. 29 - Hepatotoxicity of cardiovascular and antidiabetic drugs. In *Drug-Induced Liver Disease*, 3rd ed (eds, N. & L. D.) 519–540 (Academic, 2013).
- Babatin, M. et al. Amiodarone hepatotoxicity. *Curr. Vasc Pharmacol.* **6**, 228–236. <https://doi.org/10.2174/157016108784912019> (2008).

40. Yan, J. Y. et al. Ketoconazole associated hepatotoxicity: a systematic review and meta- analysis. *Biomed. Environ. Sci.* **26**, 605–610. <https://doi.org/10.3967/0895-3988.2013.07.013> (2013).
41. Silva, A. M. et al. Involvement of mitochondrial dysfunction in nefazodone-induced hepatotoxicity. *Food Chem. Toxicol.* **94**, 148–158. <https://doi.org/10.1016/j.fct.2016.06.001> (2016).
42. Sato, T. et al. Role of respiratory uncoupling in drug-induced mitochondrial permeability transition. *Toxicol. Appl. Pharmacol.* **427**, 115659. <https://doi.org/10.1016/j.taap.2021.115659> (2021).
43. LeCluyse, E. L. Human hepatocyte culture systems for the in vitro evaluation of cytochrome P450 expression and regulation. *Eur. J. Pharm. Sci.* **13**, 343–368. [https://doi.org/10.1016/s0928-0987\(01\)00135-x](https://doi.org/10.1016/s0928-0987(01)00135-x) (2001).
44. Guiguen-Guillouzo, C. & Guillouzo, A. General review on in vitro hepatocyte models and their applications. *Methods Mol. Biol.* **640**, 1–40. https://doi.org/10.1007/978-1-60761-688-7_1 (2010).
45. Soldatow, V. Y. et al. In vitro models for liver toxicity testing. *Toxicol. Res. (Camb)*. **2**, 23–39. <https://doi.org/10.1039/C2TX20051A> (2013).
46. Zimmermann, H. W. et al. Functional role of monocytes and macrophages for the inflammatory response in acute liver injury. *Front. Physiol.* **3**, 56. <https://doi.org/10.3389/fphys.2012.00056> (2012).
47. Cichoz-Lach, H. & Michalak, A. Oxidative stress as a crucial factor in liver diseases. *World J. Gastroenterol.* **20**, 8082–8091. <https://doi.org/10.3748/wjg.v20.i25.8082> (2014).
48. Trefts, E. et al. The liver. *Curr. Biol.* **27**, R1147–R1151. <https://doi.org/10.1016/j.cub.2017.09.019> (2017).
49. Mihajlovic, M. & Vinken, M. Mitochondria as the target of hepatotoxicity and Drug-Induced liver injury: molecular mechanisms and detection methods. *Int. J. Mol. Sci.* **23** <https://doi.org/10.3390/ijms23063315> (2022).
50. Liu, C. et al. Assessment of mitochondrial dysfunction-related, drug-induced hepatotoxicity in primary rat hepatocytes. *Toxicol. Appl. Pharmacol.* **302**, 23–30. <https://doi.org/10.1016/j.taap.2016.04.010> (2016).
51. Roghani, M. et al. Alleviation of liver dysfunction, oxidative stress and inflammation underlies the protective effect of ferulic acid in Methotrexate-Induced hepatotoxicity. *Drug Des. Devel. Ther.* **14**, 1933–1941. <https://doi.org/10.2147/DDDT.S237107> (2020).
52. Borrelli, A. et al. Role of gut microbiota and oxidative stress in the progression of non-alcoholic fatty liver disease to hepatocarcinoma: current and innovative therapeutic approaches. *Redox Biol.* **15**, 467–479. <https://doi.org/10.1016/j.redox.2018.01.009> (2018).
53. Lacour, S. et al. Cytokines as potential biomarkers of liver toxicity. *Cancer Biomark.* **1**, 29–39. <https://doi.org/10.3233/cbm-2005-1105> (2005).
54. Shakiba, E. et al. Evaluation of serum interleukin-10 levels in hepatocellular carcinoma patients: a systematic review and meta-analysis. *Clin. Exp. Hepatol.* **4**, 35–40. <https://doi.org/10.5114/ceh.2018.73484> (2018).
55. Segovia-Zafra, A. et al. Control compounds for preclinical drug-induced liver injury assessment: Consensus-driven systematic review by the ProEuroDILI network. *J. Hepatol.* **81**, 630–640. <https://doi.org/10.1016/j.jhep.2024.04.026> (2024).
56. Lala, V. et al. Liver function tests. In *StatPearls*, StatPearls Publishing Copyright © 2022, (StatPearls Publishing LLC., 2022).
57. Keshet, R. et al. Rewiring Urea cycle metabolism in cancer to support anabolism. *Nat. Rev. Cancer.* **18**, 634–645. <https://doi.org/10.1038/s41568-018-0054-z> (2018).
58. Mostafavi-Pour, Z. et al. In vitro analysis of CsA-induced hepatotoxicity in HepG2 cell line: oxidative stress and alpha2 and beta1 integrin subunits expression. *Hepat. Mon.* **13**, e11447. <https://doi.org/10.5812/hepatmon.11447> (2013).

Acknowledgements

This work was funded by a project of the Korea Research Institute of Chemical Technology (KK2341-40, SI2231-440) and the Technology Innovation Program at the Ministry of Trade, Industry and Energy (20009774).

Author contributions

D.-S.S. and H.N.J. carried out the experiments. D.-S.S. wrote the main manuscript with support from H.N.J. Both J.Y.Y. and H.N.J. prepared Figs. 1, 2, 3, 4, 5 and 6. S.J.M assisted in establishing the experimental methods. Both M.A.B. and M.J.S. conceived of the presented idea and supervised the project. H.W.K contributed to the theoretical interpretation of the data. All authors discussed the results and commented on the manuscript.

Declarations

Competing interests

The authors declare no competing interests.

Additional information

Supplementary Information The online version contains supplementary material available at <https://doi.org/10.1038/s41598-025-95071-1>.

Correspondence and requests for materials should be addressed to M.J.S. or M.A.B.

Reprints and permissions information is available at www.nature.com/reprints.

Publisher's note Springer Nature remains neutral with regard to jurisdictional claims in published maps and institutional affiliations.

Open Access This article is licensed under a Creative Commons Attribution-NonCommercial-NoDerivatives 4.0 International License, which permits any non-commercial use, sharing, distribution and reproduction in any medium or format, as long as you give appropriate credit to the original author(s) and the source, provide a link to the Creative Commons licence, and indicate if you modified the licensed material. You do not have permission under this licence to share adapted material derived from this article or parts of it. The images or other third party material in this article are included in the article's Creative Commons licence, unless indicated otherwise in a credit line to the material. If material is not included in the article's Creative Commons licence and your intended use is not permitted by statutory regulation or exceeds the permitted use, you will need to obtain permission directly from the copyright holder. To view a copy of this licence, visit <http://creativecommons.org/licenses/by-nc-nd/4.0/>.

© The Author(s) 2025